

## Observation of a Complex Multistage Transition in the JT-60U $H$ -mode Edge

K. Kamiya,<sup>1</sup> K. Ida,<sup>2</sup> Y. Sakamoto,<sup>1</sup> G. Matsunaga,<sup>1</sup> A. Kojima,<sup>1</sup> H. Urano,<sup>1</sup> N. Oyama,<sup>1</sup> Y. Koide,<sup>1</sup> and Y. Kamada<sup>1</sup>

(JT-60 Team)<sup>1</sup>

<sup>1</sup>Japan Atomic Energy Agency, JAEA, Naka, Ibaraki-ken, 311-0193, Japan

<sup>2</sup>National Institute for Fusion Science, NIFS, Toki, Gifu 509-5292, Japan

(Received 23 March 2010; published 22 July 2010)

A complex multistage transition of the edge radial electric field is observed in JT-60U  $H$ -mode phase without edge localized mode. An interesting feature is that the poloidal rotation velocity of the carbon impurity ions changes in the later  $H$ -phase without a comparable change in the main ion pressure gradient, indicating a change in the parallel momentum (and particle) balance channel.

DOI: 10.1103/PhysRevLett.105.045004

PACS numbers: 52.55.Fa, 52.25.Fi, 52.50.Gj

Since the high confinement mode regime ( $H$ -mode) was discovered in the ASDEX tokamak [1], the physics of transitions from the low confinement mode ( $L$ -mode) to the  $H$ -mode ( $L$ - $H$  transition) has attracted a great deal of interest in the both the experimental and theoretical communities [2–5].

Experimentally, the radial electric field  $E_r$  was observed in a localized region just inside the separatrix of most  $H$ -mode plasmas where the sheared  $ExB$  flow was created and where the fluctuations decreased. On the theory side, the suppression of turbulence by  $ExB$  velocity shear proposed by Shaing [2] could lead to a spontaneous  $H$ -mode bifurcation through a nonlinear feedback [6]. However the relationship between the mechanism of formation of the edge transport barriers and  $ExB$  shear is not well understood, since it is related to a nonlinear dynamics in the edge plasma.

The very high confinement mode regime ( $VH$  mode) first observed on DIII-D is characterized by a “two-stage” transition with a typical  $H$  mode followed much later in the  $H$  mode phase without edge localized mode (ELM-free) by a second increase in the energy confinement [7]. In the case of the  $VH$  mode on DIII-D, the toroidal rotation played an important role in the second phase but a similar phenomenon was observed on joint European torus (JET) with only rf heating [8].

Recently 32 spatial channel charge exchange recombination spectroscopy CXRS with fast time-resolution up to 400 Hz has been installed on JT-60U [9]. Since the transition between the internal transport barriers with different curvature of ion temperature (or “multiple levels” of reduced transport) in reversed shear plasmas was discovered in the plasma core region [10,11], similar phenomena must exist even in the edge transport barriers region.

This Letter provides new information on the phenomenology of a complex multistage transition in terms of the

edge radial electric field in the  $H$ -mode discharge on JT-60U. The data presented here fall within the range of  $H$ -mode and  $VH$ -mode phenomenology [12]. The slowness of the first  $L$ - $H$  transition without any bursts in the  $D_\alpha$  signal is also found [13], and a complex multistage transition in the later ELM-free  $H$  phase is sequentially followed, which is not observed on DIII-D or JET. A slow  $L$ - $H$  transition had been seen on DIII-D (dubbed the  $IM$  mode [14]), although the  $IM$  mode is characterized by periodic bursts of an instability near the outer plasma edge.

The radial electric field, pressure gradient, and plasma velocity perpendicular to the magnetic field are governed by the radial force balance equation:  $E_r = (Z_j e n_j)^{-1} \nabla p_j - V_{\theta,j} B_\phi + V_{\phi,j} B_\theta$ . Here,  $Z_j$  is the ion charge,  $n_j$  is the ion density,  $e$  is the magnitude of the electron charge,  $p_j = n_j T_j$  is the ion pressure with  $T_j$  the ion temperature,  $V_{\theta,j}$  and  $V_{\phi,j}$  are the ion poloidal and toroidal rotation velocities, respectively, and  $B_\theta$  and  $B_\phi$  are the poloidal and toroidal magnetic fields, respectively.

Figure 1 shows a time evolution of the balanced neutral beam injection (NBI) heating discharge having a two step transition with  $P_{NB} = 10$  MW (E049219;  $I_p \sim 1.6$  MA,  $B_\phi \sim 3.9$  T,  $q_{95} \sim 4.2$ ,  $\kappa/\delta \sim 1.43/0.34$  at  $t \sim 5.0$  sec). It is clear that the  $L$ - $H$  transition occurs spontaneously at  $t \sim 4.730$  sec, indicating an abrupt drop in the  $D_\alpha$  emission in addition to an increase in the time differential in the line-averaged electron density. The plasma exhibits a “slow” transition within a time scale of about  $\sim 50$  ms as the ion temperature and its gradient buildup associated with the  $E_r$ -well formation at around the maximum  $|\nabla T_i|$  location as shown in Fig. 2.

A “faster” drop in the  $D_\alpha$  emission within less than a few millisecond can be seen at  $t \sim 5.0525$  sec, exhibiting a rapid change in the  $E_r$ -well structure toward more negative by approximately a factor of 2. After a brief improved

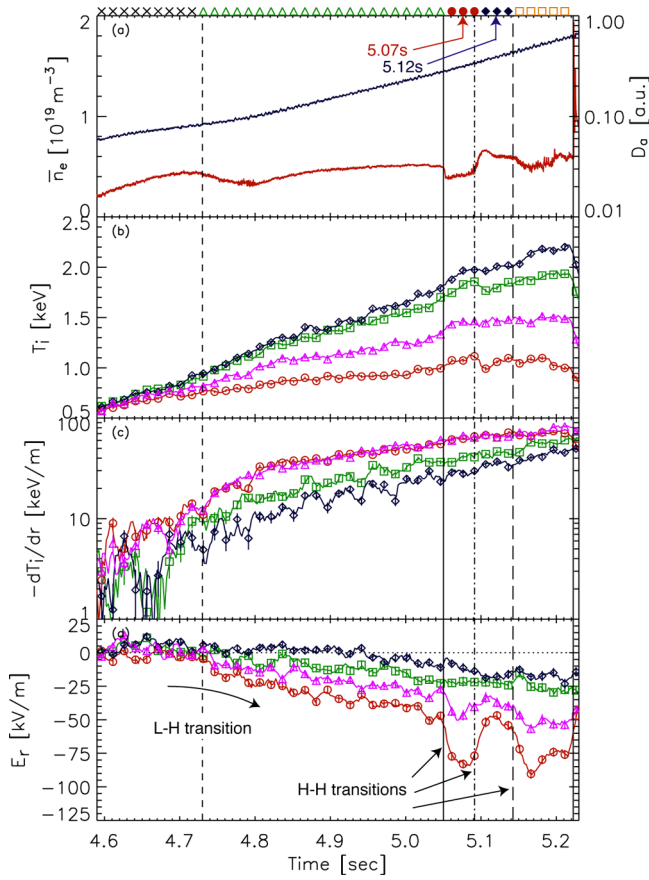


FIG. 1 (color online). Temporal evolution of (a) line-averaged electron density and  $D_\alpha$  emission, (b) ion temperature  $T_i$ , (c) ion temperature gradient  $-\nabla T_i$ , and (d) radial electric field  $E_r$  for  $\sim 3.4$  cm [(red) circles],  $\sim 3.9$  cm [(orange) triangles],  $\sim 4.5$  cm [(green) squares], and  $\sim 5.1$  cm [(blue) diamonds] inside the separatrix. The times of the  $L$ - $H$  and  $H$ - $H$  transitions are indicated by vertical lines.

confinement phase, a deeper negative  $E_r$ -well structure is back to a shallower one at  $t \sim 5.0925$  sec. The  $E_r$  transition towards more negative occurs again at  $t \sim 5.1425$  sec, indicating a complex multistage transition (called “ $H$ - $H$ ” transition). An interesting feature of this observation is that the poloidal velocity of the carbon changes in the later  $H$  phase without a comparable change in the ion pressure profile as shown in Fig. 3.

The edge  $E_r$  well at the initial  $H$  phase (just after a  $L$ - $H$  transition of  $t \sim 4.73$ – $5.05$  sec) is maintained by the both diamagnetic  $\nabla p_i / (Z_j e n_i)$  and poloidal velocity  $-V_\theta B_\phi$  terms for the carbon impurity ions ( $Z_j = 6$ ) with an almost similar magnitude of up to  $-20$  kV/m. It is noted that the poloidal velocity for the carbon impurity ions is in the electron diamagnetic direction, and the toroidal rotation goes towards counter direction to the plasma current. Although both poloidal and toroidal velocity terms contribute to the negative  $E_r$  formation, the contribution of the toroidal velocity term is less than a half of the poloidal velocity term. Because the NBI torque is balanced in this

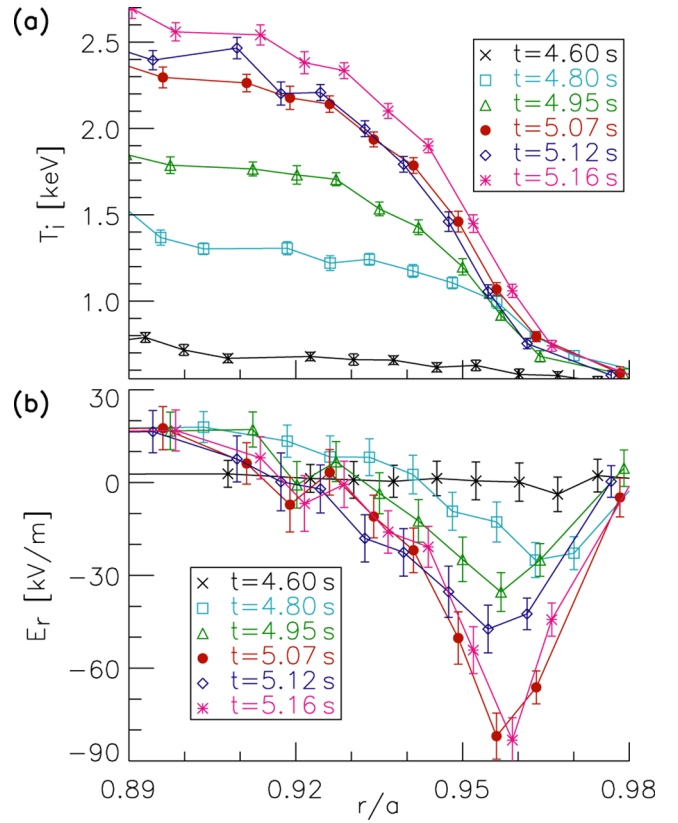


FIG. 2 (color online). Plot of (a) ion temperature and (b) radial electric field versus normalized radius for  $t = 4.6$  [(black) crosses],  $4.8$  [(sky-blue) squares],  $4.95$  [(green) triangles],  $5.07$  [(red) circles],  $5.12$  [(blue) diamonds], and  $5.16$  s [(pink) asterisks].

discharge, the change of the toroidal velocity term associated with the increase in the diamagnetic term is considered to be a “spontaneous” toroidal rotation.

The change in the  $E_r$  well toward more negative (up to  $-80$  kV/m) can be seen in the later  $H$  phase at  $t \sim 5.05$  sec, which is associated with the dominant poloidal velocity term for the carbon impurity ions without a comparable change in both the diamagnetic and toroidal velocity terms. This indicates a change in the parallel (poloidal) momentum balance channel. After a brief backward  $H$ - $H$  transition ( $t \sim 5.0915$ – $5.1425$  sec), the poloidal velocity term changes solely at  $t \sim 5.1425$  sec (2nd  $H$ - $H$  transition), again, in the latest  $H$ -phase until the first large ELM onset at  $t \sim 5.2225$  sec.

This interpretation is complicated by Fig. 4 that shows the electron density gradient changes slightly in concert with the  $E_r$  (or  $ExB$  shear) change. Hence, the main ion density gradient (not measured) must also change, since we could see a slight change in the measured carbon ion density. Because of this change in electron density gradient, it is hard to rule out a change in the particle transport contributing to the deepening of the  $E_r$  well. This would most likely be both a momentum and particle transport change.

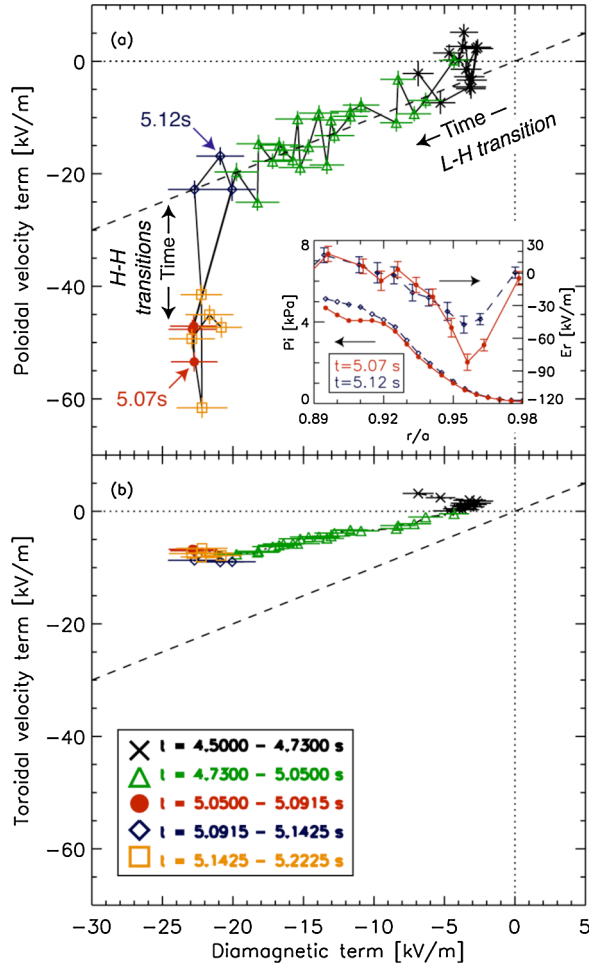


FIG. 3 (color online). Contributions of (a) poloidal ( $-V_\theta B_\phi$ ) and (b) toroidal ( $-V_\phi B_\theta$ ) velocity terms to the  $E_r$  in the radial force balance equation plotted as a function of diamagnetic term  $[\nabla p_i / (Z_i e n_i)]$  for the measured carbon impurity ions at  $\sim 3.4$  cm inside the separatrix. These data are smoothed by every 15 ms from  $t \sim 4.53625$  sec to  $t \sim 5.22625$  sec. Radial profiles of the calculated pressure of main ion with assumption that the edge deuterium ion density  $n_i \approx$  the edge electron density  $n_e$  [the pressure gradient term can be estimated as  $\nabla(n_i T_i) \approx \nabla(n_e T_i)$ ] and electric field at  $t \sim 5.07$  sec and 5.12 sec are also plotted.

There are three stages in the later  $H$ -mode phase in terms of the  $E_r$  transition, where the density or temperature gradient gradually change in time as shown in Fig. 4. It is noted that there is no simple relation to the change in  $ExB$  shear. After a  $L$ - $H$  transition, both density and temperature (and hence, pressure) gradient increase as the  $ExB$  shear increases up to  $\sim 1$  MHz. However, only the density gradient increases without a comparable change in the temperature gradient at the first  $H$ - $H$  transition, even as the  $ExB$  shear increases by a factor of 2 (up to  $\sim 2$  MHz). At the following backward  $H$ - $H$  transition, it is interesting that the density gradient decreases and temperature gradient increases, while the pressure gradient is kept almost

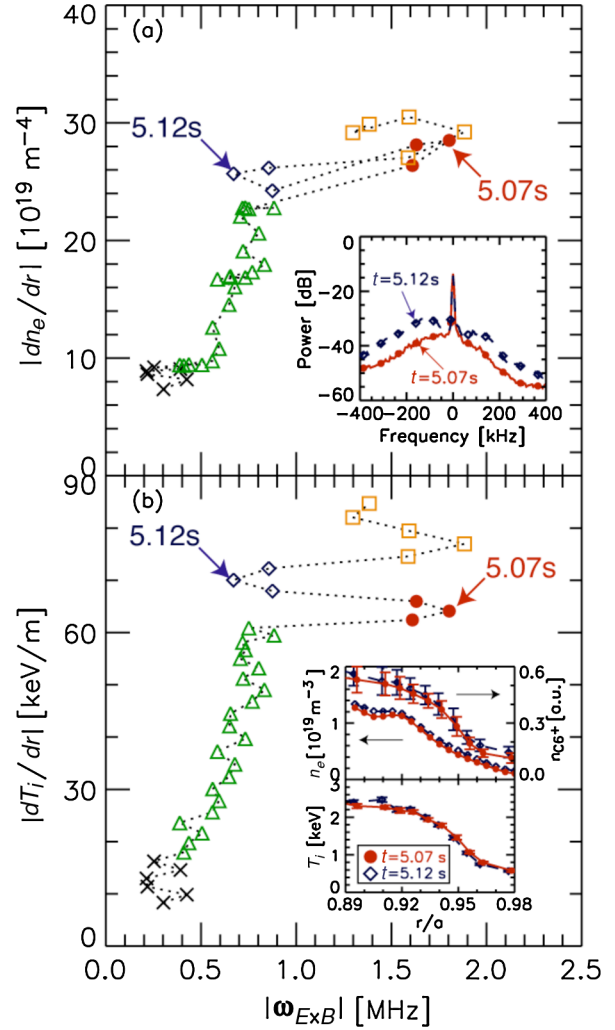


FIG. 4 (color online). (a) Electron density and (b) ion temperature gradients at  $\sim 3.9$  cm inside the separatrix plotted as a function of  $ExB$  shear [defined by  $\omega_{ExB} = (r/q)d\{q/r\}\{E/B\}/dr$ ]. Power spectrum of electron density fluctuation measured by reflectometer (cut-off density  $n_e^{\text{cut-off}} \sim 1.4 \times 10^{19} \text{ m}^{-3}$ ) at  $t \sim 5.07$  sec and 5.12 sec are plotted in (a). Radial profiles of electron density,  $n_e$  measured by Li-beam probe (LiBP), ion density,  $n_{C6+}$ , and ion temperature,  $T_i$ , for carbon impurity ions measured by CXRS are also plotted in (b).

constant. In this backward transition, the density fluctuation at the plasma edge region is enhanced, which is consistent with an enhanced particle transport according to the decrease in the  $ExB$  shear. This observation suggests that the particle transport ( $\approx |dn_e/dr|$ ) may be directly related with the  $ExB$  shear even in the later  $H$  phase, while a stronger  $ExB$  shear (above  $\sim 1$  MHz in this experimental case) seems not to be directly related to an improvement in the energy transport ( $\approx |dT_i/dr|$ ). The mechanism, which leads to the occurrence of a complex multistage transition, is not well understood yet; although the plasma instability (such as observed density fluctuations having broadband spectrum in the frequency range of 100–400 kHz) driven

by the free energy of the radial shear in the parallel (poloidal) velocity may play an important role [15].

This work was supported in part by Grant-in-Aid for Young Scientist (A) 19686056.

- 
- [1] F. Wagner *et al.*, *Phys. Rev. Lett.* **49**, 1408 (1982).
  - [2] K. C. Shaing and E. C. Crume, Jr., *Phys. Rev. Lett.* **63**, 2369 (1989).
  - [3] R. J. Groebner *et al.*, *Phys. Rev. Lett.* **64**, 3015 (1990).
  - [4] K. Ida *et al.*, *Phys. Rev. Lett.* **65**, 1364 (1990).
  - [5] R. A. Moyer *et al.*, *Phys. Plasmas* **2**, 2397 (1995).
  - [6] F. L. Hinton and G. M. Staebler, *Phys. Fluids B* **5** 1281 (1993).
  - [7] G. L. Jackson *et al.*, *Phys. Rev. Lett.* **67**, 3098 (1991).
  - [8] M. Greenfield *et al.*, *Plasma Phys. Controlled Fusion* **35** B263 (1993).
  - [9] K. Ida *et al.* *Rev. Sci. Instrum.* **79**, 053506 (2008).
  - [10] Y. Sakamoto *et al.*, *Nucl. Fusion* **44**, 876 (2004).
  - [11] K. Ida *et al.*, *Phys. Rev. Lett.* **101**, 055003 (2008).
  - [12] G. M. Staebler *et al.*, *Phys. Plasmas* **1**, 909 (1994).
  - [13] M. Kikuchi *et al.*, in *Proc. 20th European Conf. on Control Fusion and Plasma Phys, Lisbon, 1993* (EPS, Petit-Lancy, Switzerland, 1993), Part 1, p. 179.
  - [14] R. J. Colchin *et al.*, *Phys. Rev. Lett.* **88**, 255002 (2002).
  - [15] R. H. Cohen *et al.*, *Contrib. Plasma Phys.* **34**, 232 (1994).